Materials Science & Engineering A 832 (2022) 142444

Contents lists available at ScienceDirect

Materials Science & Engineering A

journal homepage: www.elsevier.com/locate/msea

Microstructure evolution and mechanical properties of continuous drive friction welded dissimilar copper-stainless steel pipe joints

Hardik D. Vyas [a], Kush P. Mehta [a,b,*], Vishvesh Badheka [a], Bharat Doshi [c]

[a] Department of Mechanical Engineering, School of Technology, Pandit Deendayal Energy University, Raisan, Gandhinagar, Gujarat, India
[b] LUT Mechanical Engineering, School of Energy Systems, LUT University, Yliopistonkatu 34, Lappeenranta, 53850, Finland
[c] Institute for Plasma Research, Gandhinagar, Gujarat, India

ARTICLE INFO

Keywords:
Dissimilar joints
Friction welding
Mechanical properties
Microstructure
Pipe joints
Reaction layer

ABSTRACT

In the present investigation, the microstructure evolution and mechanical properties of dissimilar materials Copper-Stainless Steel pipe joints welded by continuous drive friction welding under two different processing conditions are analyzed. The processing conditions of friction welding for copper-stainless steel joints are varied by two friction times of 10 s and 15 s while keeping other processing parameters constant. The welded specimens are analyzed for materials characterizations and mechanical testing using optical microscopy and scanning electron microscopy, electron dispersive x-ray spectroscopy, electron backscatter diffraction analysis, X-ray diffractions, tensile testing, and microhardness measurements. The results revealed that the major microstructural evolution is observed at the Cu side with dynamic recrystallized zones. Enhanced metallurgical bonding between Cu-SS materials is obtained with microstructural evolutions (such as full dynamic recrystallized zone at Cu side and quenching zone at SS side) near to Cu-SS interface, in case of weld made by friction time of 15 s. Superior interatomic diffusion leading to enhanced metallurgical bonding is evidenced for weld made by friction time of 15 s. The reaction layer thickness influences the bonding and mechanical properties of Cu-SS friction welds. The reaction layer thickness of 17.28 μm is observed for the weld made by friction time of 10 s, whereas the reaction layer thickness of 1.21 μm is observed for the weld made by friction time of 15 s. The ultimate tensile strength of 181.05 MPa is obtained for Cu-SS friction weld.

1. Introduction

Dissimilar welding of copper (Cu) to stainless steel (SS) combination is one of the best engineering solutions in multi-materials processing due to advantages of cost reduction with enhanced system performance by having hybrid properties at two different sides. This Cu-SS combination has already been applied to different engineering applications in the fields of cryogenics, aerospace, automobiles, nuclear, and reactors systems [1–6]. However, Cu and SS materials have different chemical, and physical properties, and hence, it is very challenging to obtain sound metallurgical joints in case of hybrid system of Cu to SS materials welding. Considering these challenges, fusion welding processes are not recommended for welding of Cu-SS dissimilar materials, whereas solid-state welding processes are considered as one of the most feasible solutions for dissimilar materials welding [7–10], including Cu-SS system [11–13]. Friction welding (FW) is a solid-state welding process that has already proved feasibility to weld different dissimilar materials' combinations. FW is applied on Cu to SS combination in different previous studies. Shanjeevi et al. [14] have investigated 24 mm solid rod diameter of austenitic SS to Cu joint using the FW process. They have optimized the FW process parameters, and have received 229 MPa joint strength. In another study by Shanjeevi et al. [15] for Austenitic SS to Cu with 24 mm diameter of solid bar, it is claimed that the process parameters of FW such as rotation speed, friction pressure, and upset pressure influence joint strength. They have reported that a maximum of 238 MPa joint strength can be obtained. FU et al. [16] have performed a study on continuous drive friction welding for T2 Cu to 1Cr18Ni9Ti SS materials having a 30 mm solid rod diameter. They have obtained the highest torsional strength using an additional electric field during processing of FW. Luo et al. [17] have investigated the inertia radial friction welding process for dissimilar H90 Brass to D60 steel materials having 156 mm solid rod diameter. They have performed a little study on the microstructure of welded specimens and found that bainite and martensite were developed in the thermo-mechanical affected zone (TMAZ). Sahin et al. [18] have investigated the continuous drive FW

* Corresponding author. Department of Mechanical Engineering, School of Technology, Pandit Deendayal Energy University, Raisan, Gandhinagar, Gujarat, India.
E-mail addresses: kush.mehta@lut.fi, kush_2312@yahoo.com (K.P. Mehta).

https://doi.org/10.1016/j.msea.2021.142444
Received 23 October 2021; Received in revised form 29 November 2021; Accepted 30 November 2021
Available online 2 December 2021

Abbreviations

Electrolytic tough pitch copper ETP-Cu
Stainless steel SS
Quenching zone QZ
Full dynamic recrystallization zone FDRZ
Partial dynamic recrystallization zone PDRZ
Base metal BM
Revaluation per minutes RPM
Electron backscatter diffraction EBSD
Scanning electron microscopy SEM
Electron dispersive x-ray spectroscopy EDS
X-ray diffraction analysis XRD
Intermetallic compound IMC

Table 1
Chemical composition of base metals.

SS 304L	C	Mn	Si	Cr	Ni	P	S	Fe
wt. %	0.028	1.14	0.36	18.36	8.2	0.026	0.002	Balance
ETP-Cu	Cu		Pb		P		Si	
wt. %	Balance		0.002		0.005		0.005	

2. Materials and methods

In this investigation, the friction welding of pipe materials such as electrolyte tough pitch copper (ETP-Cu (Cu)) and stainless-steel alloy 304L (SS) are performed using a continuous drive friction welding machine (make of ETA Technology). Fig. 1 provides information on the dimensions of pipes and their position in the machine like the SS pipe is fixed in the rotating chuck, while the Cu pipe is kept stationary on the opposite side. Table 1 and Table 2 present the chemical compositions, and mechanical and physical properties of the base materials

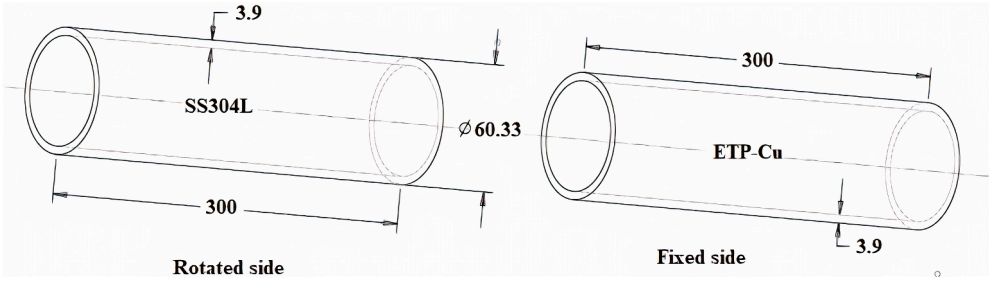

Fig. 1. Dimensions of pipes and position in friction welding machine.

process for dissimilar AISI304 SS to Cu materials consisting of 10 mm of rod diameter. They have claimed that friction pressure and friction time influence joint strength and the formation of intermetallic compounds (IMCs). Tsuchiya et al. [19] have performed FW on dissimilar materials of Cu–Cr–Zr alloy to SS316 consisting of 25 mm rod diameter. They suggested that optimized process parameters of FW can lead to maximum joint strength. They have considered rotational speed, friction pressure, upset pressure, and welding time as FW process parameters in their study. Vairamani et al. [20] have studied FW on the solid rod for dissimilar materials of Austenitic SS 304 to Cu. They have also worked on optimization for FW parameters to obtain maximum joint strength. Vyas et al. [5,21,22] have studied two different dissimilar materials' joints (of Al-SS and Cu-SS), wherein they studied pipe joint configuration for welding parameters, non-destructive tests of welds, and welds' properties.

Considering the articles on FW for dissimilar Cu-SS joints, the published articles are majorly on FW process parameters and their optimization to obtain maximum joint strength. Also, most of them are investigated for solid rod configuration, and there is only one recent article that was studied for pipe joint configuration of Cu-SS FW. There is no systematic analysis performed that studies microstructural growth after FW in case of Cu-SS pipe joints. The microstructure evolution under different processing conditions of FW is also not investigated so far. Additionally, the correlation between FW processing-microstructure evolution-joint properties is very much interesting to establish scientific understanding, which is hitherto not investigated systematically in case of Cu-SS FW joints. Therefore, it is worthwhile to study microstructure evolution and mechanical properties of continuous drive friction welded dissimilar Cu-SS pipe joints. In the present investigation, microstructure variations at the interface region and mechanical properties of Cu-SS pipe FWed joints (welded under two different conditions varied by two different friction times) are analyzed and correlated.

respectively.

The experiments are performed considering two different conditions of friction times keeping other processing parameters constant. The friction time is kept at 10 s for the first experimental condition, while 15 s for the second experimental condition. The rest of the parameters such as rotational speed of 350 RPM, friction pressure of 27.58 MPa, upset time of 5 s, and upset pressure of 55.16 MPa are kept constant. The selection of the welding parameters is considered based on the understanding developed through our previous studies [5,21,22], and experimental trials. Before the FW processing, the mating surfaces of Cu and SS are properly cleaned by applying acetone to remove impurities from the surfaces. At the end of the FW experiments, the burn-off length (BOL) is measured as 12.73 mm and 18.62 mm for the first experiment and second experiment respectively. The differences in the formation of flash with burn off length can be correlated from Fig. 2. It can be seen that high amount of flash is formed for weld made by friction time of 15 s as can be seen from Fig. 2 (c & d) as compared to weld made by friction time of 10 s.

After performing welding, the welded samples are subjected to materials characterizations and mechanical testing, which are performed using optical microscopy and scanning electron microscopy (SEM) & electron dispersive x-ray spectroscopy (EDS), Electron back scatters analysis (EBSD) X-ray diffractions (XRD), tensile testing and microhardness measurements.

The optical microscopy is performed using an Olympus microscope of BX53 M model, wherein the samples are processed according to the standard metallurgical procedures such as mounting, polishing, and chemical etching with etchant reagent of aqua regia (70% HNO_3 and 30% HCL) applied at SS side of material and potassium dacromet (99.99%) applied at Cu side of the material. The grain formation, variations, and interlayer thickness are investigated at the weld interface region. EBSD is performed at the interface region to further analyze grain variations with more detailed information and analysis. EBSD is performed on Keyence, Quanta 3D FEG microscope. SEM and EDS are

Table 2
Mechanical and physical properties of base metals.

Base materials	Yield strength, MPa	Ultimate tensile strength, MPa	% Elongation	Melting point °C	Thermal conductivity W/m*k	Specific heat J/kg*K
SS 304L	206	517	76.56	1454	16.2	500
ETP-Cu	228.89	286.17	20.34	1083	390	386

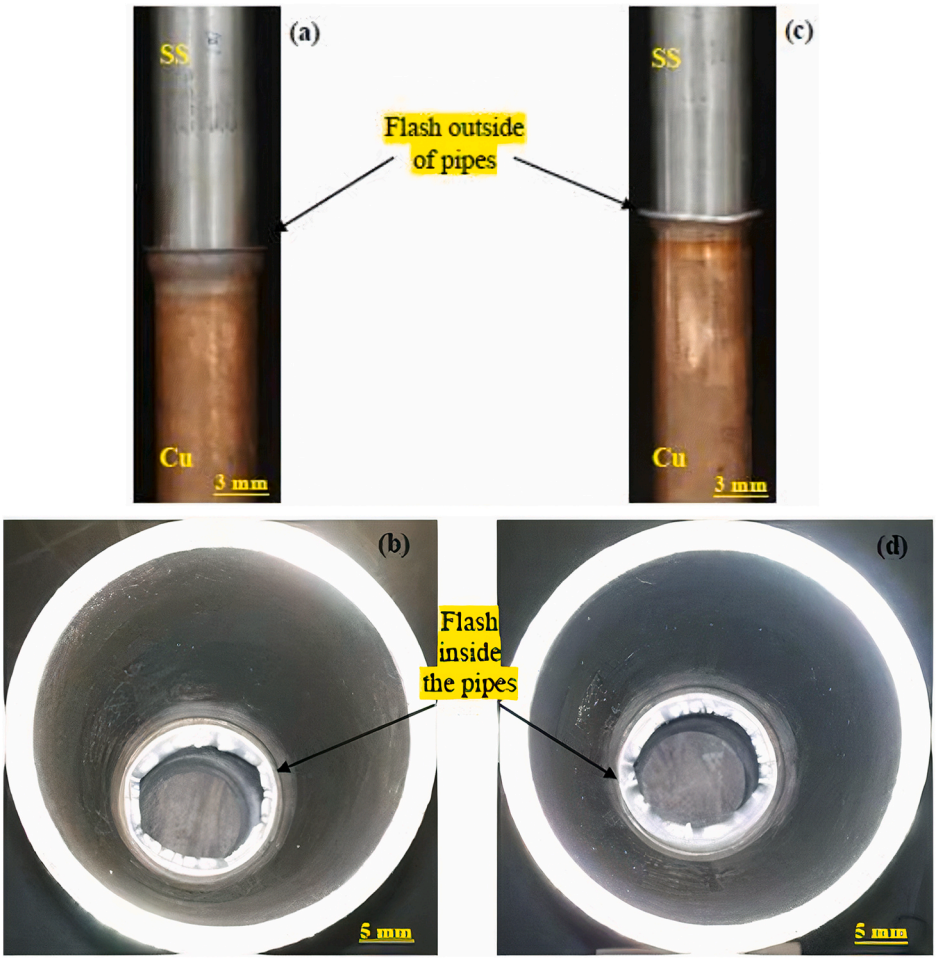

Fig. 2. Welded specimens showing flash formation for two conditions (a & b) weld made by friction time of 10 s and (c & d) weld made by friction time of 15 s.

performed at the interface region using ZEISS SEM 360 machine to identify the elemental distribution and to analyze bonding between dissimilar materials. The XRD is performed on the 8.0-Bruker machine to identify the IMCs.

The tensile testing is performed after extracting tensile specimens from welded samples. The extraction of samples is performed using wire-cut electric discharge machining along the transverse direction of the pipe joints as per the standard dimensions mentioned in Section IX of American Society of Mechanical Engineers (ASME) standards, as shown in Fig. 3. For the tensile testing, 1 mm/min crosshead travel speed is used, and the test is performed using Universal Testing Machine (make Krutam Techno-FSA/M – 100 model). The fractured tensile surfaces are further investigated by SEM (using a machine of ZEISS, Model SEM 360). The microhardness test is conducted using hardness measurement tester (make NEXUS 4302 model of ESEWAY machine), wherein a load of indentation is kept at 300 g, and the measurements are carried out at every 100 μm distances.

3. Results

3.1. Microstructure (optical microscopy)

Figs. 4 and 5 show the microstructure images by optical microscopy for Cu-SS friction welded specimens at friction time 10 s and 15 s respectively. Fig. 4 (a) and Fig. 4 (b) show the base metal's microstructure of SS and Cu respectively, wherein the SS microstructure shows an austenitic type structure with twin-grain boundaries, and the Cu microstructure shows smaller sized deformed grains as compared to SS.

From Fig. 4 (d) and Fig. 5 (d), it can also be seen that there is a difference in the interface thickness for two different investigated conditions of welds. In Fig. 4 (d) and Fig. 5 (d), the dark color of an interface between Cu-SS can be interpreted as either an oxide layer or a reaction layer consisting of IMCs. This reaction layer is further measured and analyzed in Fig. 6, with high magnification images.

It can be seen from Figs. 4 and 5 that microstructural changes are observed at the interface region. The Cu side of the interface region has resulted in more differences in microstructure as compared to the SS

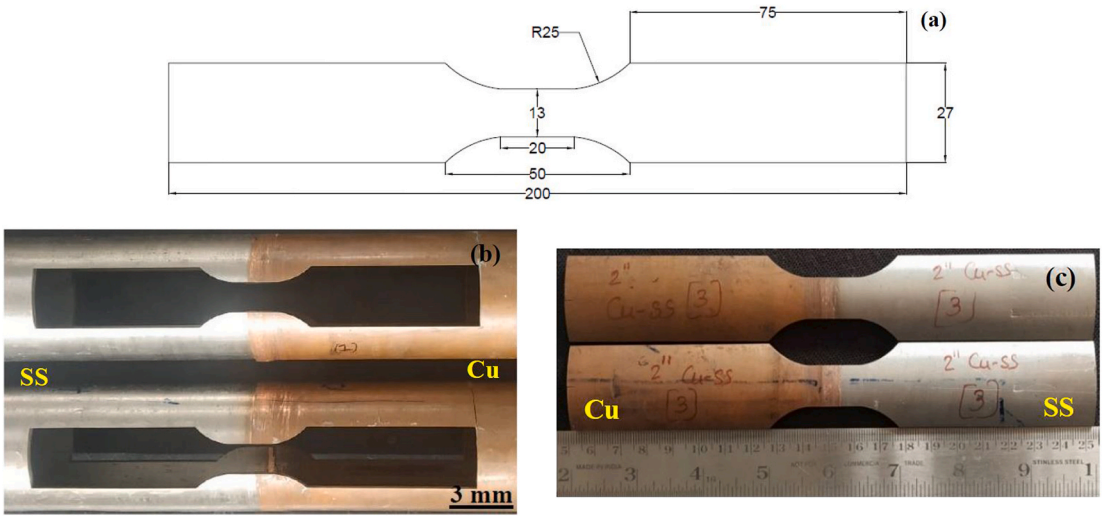

Fig. 3. (a) Tensile specimen dimensions as per standard of ASME Section IX, (all the dimensions are in mm) (b) photographs of welded pipes after extraction of tensile specimens (c) photograph of extracted tensile specimens.

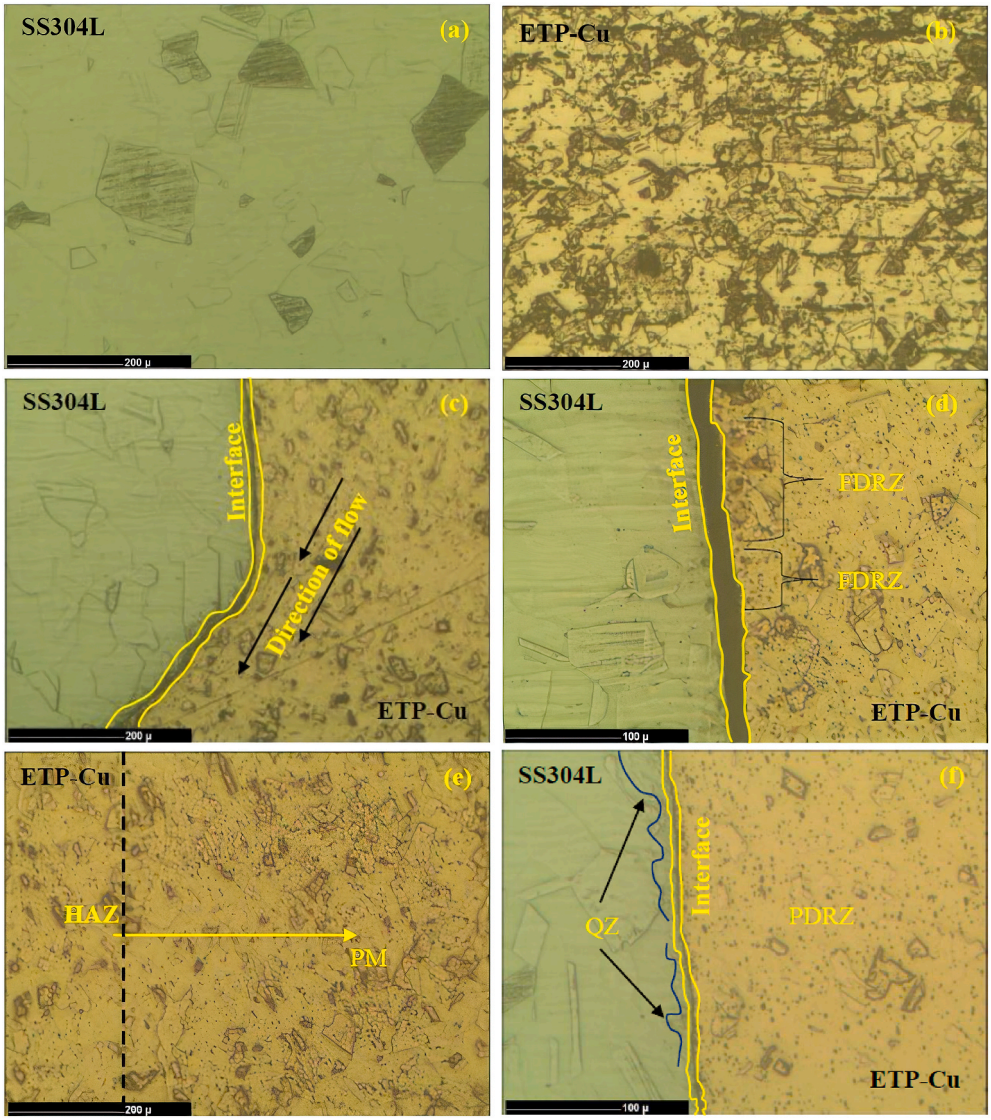

Fig. 4. The microstructure images of the base metals and Cu-SS joint welded at friction time of 10 s; (a) SS base metal; (b) Cu base metal; (c) Cu-SS interface showing Cu grain structure; (d) Cu-SS interface showing FDRZ; (e) Cu side showing HAZ to PM; (f) Cu-SS interface showing PDRZ at Cu side and QZ at SS side.

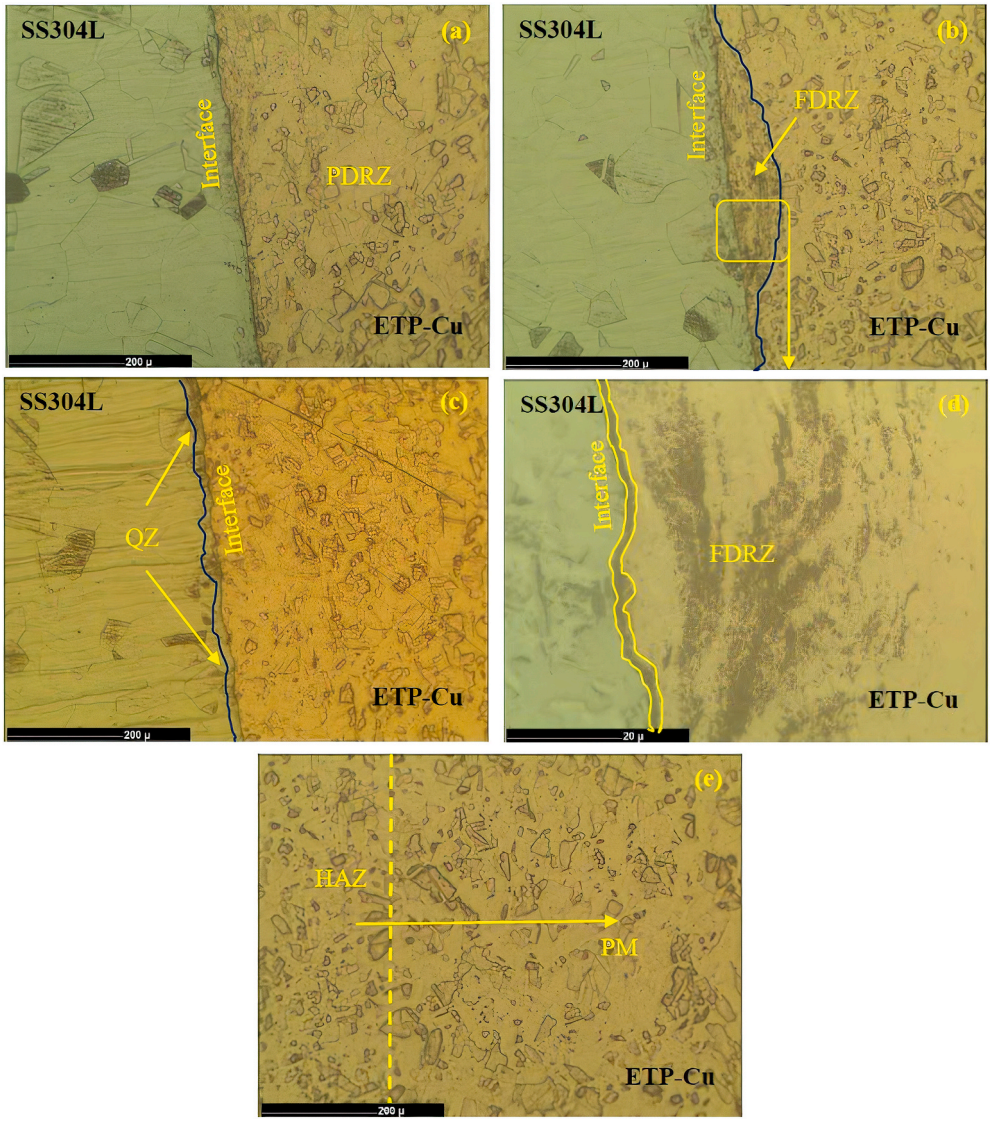

Fig. 5. The microstructure images of Cu-SS joint welded at friction time of 15 s; (a) Cu-SS interface showing PDRZ; (b) Cu-SS interface showing FDRZ; (c) Cu-SS interface showing QZ at SS side; (d) higher magnification image of region d shown at image b, showing FDRZ at Cu side near to Cu-SS interface; (e) Cu side showing HAZ to PM.

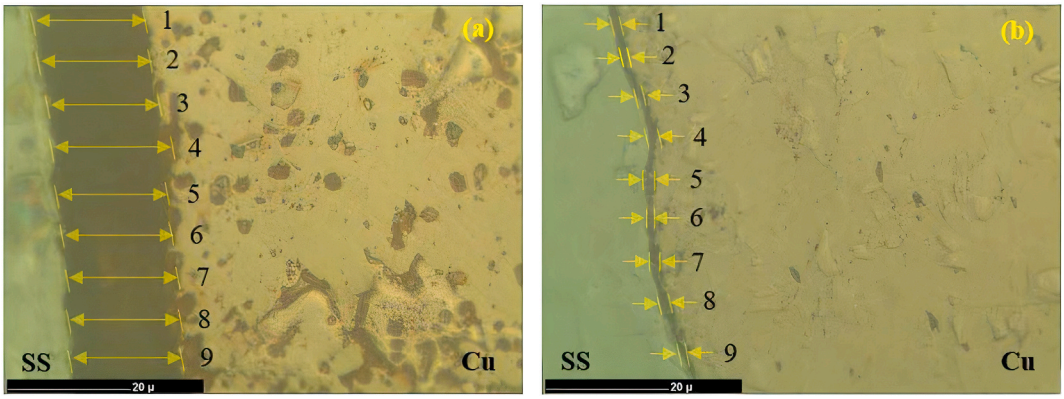

Fig. 6. Microstructure images showing measurements of reaction layer for Cu-SS joint welded at (a) friction time of 10 s and (b) friction time of 15 s.

side. The Cu side near the interface is observed with two different microstructures such as the full dynamic recrystallization zone (FDRZ) and the partial dynamic recrystallization zone (PDRZ), (refer Fig. 4 (c)–(f) and Fig. 5 (a) to (e)). Besides, there are some minor changes in microstructures observed at the SS side as can be seen from Fig. 4 (f) and Fig. 5 (c), which are interpreted as quenching zone (QZ) as those can be

Table 3
Reaction layer thickness measurements in (μm) for locations are shown in Fig. 5.

Sr.No.	Locations corresponding to Fig. 5 (a)	Locations corresponding to Fig. 5 (b)
1	16.8	1.33
2	18	1.46
3	16.93	1.33
4	17.6	1.06
5	17.73	0.93
6	17.2	1.06
7	16.4	1.33
8	17.2	1.2
9	17.73	1.2
Average	17.28	1.21

because of quenching. A similar observation on the formation of QZ is noted in another article of [23].

In the case of PDRZ, the grains are observed as partially deformed and recrystallized. In the case of weld made by friction time of 10 s, the PDRZ is observed more pronounced with elongated grains flowing towards the direction of flash as can be seen from Fig. 4 (c). Besides, the PDRZ is also observed in the case of weld made by friction time of 15 s as can be seen from Fig. 5 (a), but the grain elongation towards the direction of flash is not distinctly observed like it is observed in Fig. 4 (c). Besides, FDRZ is observed as more pronounced in the case of weld made by friction time of 15 s (Fig. 5 (b) and (d)), as compared to the weld made by friction time of 10 s (Fig. 4 (d)). This is because of differences in friction times.

Fig. 6 shows the microstructure images with differences in the thickness of the reaction layer for Cu-SS joint welded at (a) friction time of 10 s and (b) friction time of 15 s. The measurements are carried out to measure thickness at 9 different locations as shown in Fig. 6, and corresponding values of measurements are shown in Table 3. It can be seen that there is a big difference in thickness at the interface. The average width of the reaction layer is observed as 17.28 μm for weld made by friction time of 10 s, whereas it is 1.21 μm for weld made by friction time of 15 s.

3.2. Electron backscatter diffraction (EBSD) analysis at the interface zone, scanning electron microscopy (SEM), energy-dispersive X-ray spectroscopy (EDX)

Fig. 7 presents the EBSD images of base materials such as (a) ETP-Cu and (b) SS304L. The average grain size of the Cu and SS are noted as 21.3 μm and 29.9 μm respectively. It can be again confirmed clearly from these images that the SS microstructure shows twin-grain borders in typical an austenitic type structure, and the Cu microstructure shows smaller-sized deformed grains that also have a presence of twin grains.

Fig. 8 presents the EBSD images and elemental color mapping images for the interface region of two different weld conditions of 10 s friction time and 15 s friction time. It can be seen that the interface layer (i.e. reaction layer) is thick in case of weld interface of 10 s friction time (Fig. 8 (a)&(b)), which can be observed as a non-indexed region at the interface. Besides, the interface layer is thin in case of weld interface of 15 s friction time (non-indexed region at the interface in Fig. 8 (e)&(f)). Moreover, it can be seen from Fig. 8 (e)&(f) that there is a distinct FDRZ region at Cu side near to interface and QZ at SS side near to interface observed, whereas no such distinct regions are observed in the case of Fig. 8 (a)&(b). Both FDRZ and QZ of Fig. 8 (e)&(f) show recrystallized equiaxed fine grains that have occurred after severe plastic deformation by thermo-mechanical action caused by friction welding between Cu and SS. These microstructural changes are observed continuously throughout the interface region with specific width in case of weld made by friction time of 15 s, which in turn shows adequate thermo-mechanical processing between Cu and SS materials under the effect of 15 s of friction time along with other processing parameters of friction welding. In these FDRZ and QZ of Fig. 8 (e)&(f), some of the grains are not properly indexed which is may be because of severe plastic deformation. Besides, in case of weld made by friction time of 10 s, inadequate thermo-mechanical processing between Cu and SS materials is evidenced as no distinct microstructural changes at the interface such as FDRZ and/or QZ, or any other distinct microstructural change (near to Cu-SS interface) can be observed in Fig. 8 (a)&(b). This is due to inadequate thermo-mechanical processing caused by an ineffective friction time of 10 s along with investigated process parameters, which in turn resulted in improper materials mixing at the interface. The improper interfacial materials mixing can also be interpreted through elemental mapping images as shown in Fig. 8 (c)&(d) for weld made by friction time of 10 s and Fig. 8 (g)&(h) for weld made by friction time of 15 s. Fig. 8 (c)&(d) show sharp straight interface with color differences, whereas Fig. 8 (g)&(h) show wave-like interface with color differences. The inverse pole figure (IPF) of EBSD images of Fig. 8 is shown in Fig. 9, which shows that in the case of FDRZ of Fig. 8 (e)&(f), most of the grains have (101), and severely deformed grains are not indexed. In the case of QZ of Fig. 8 (e)&(f), the majority of the grains have in-between (001) and (111), wherein severely deformed grains are observed as non-indexed grains.

Fig. 10 is showing the misorientation angle from EBSD images presented in Fig. 8. An average angle from grain boundaries is considered for misorientation angle approximately 30° for both conditions. It can be seen that the misorientation angle is varied in-between 2.6° to 63.4° in case of weld made by friction time of 10 s while the same is in-between 2.5° to 61.2° in case of weld made by friction time of 15 s.

The average grain size measurements are presented in Fig. 11 for EBSD images of Fig. 8. It is observed that the average grain size of Cu

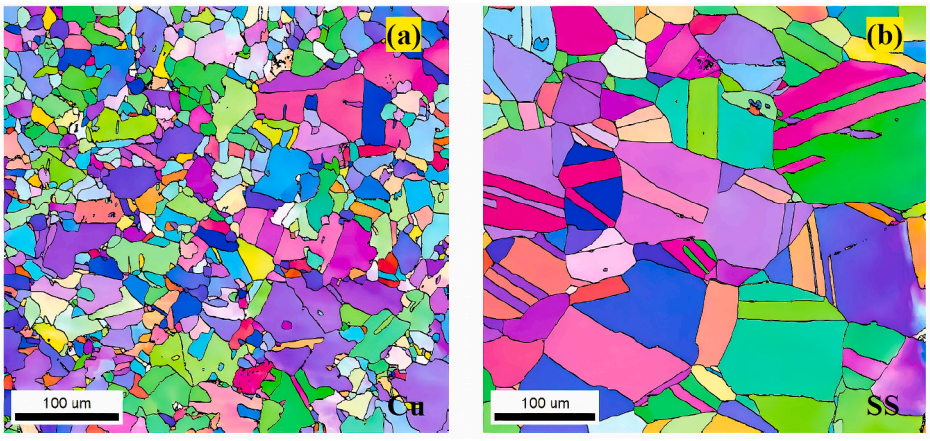

Fig. 7. EBSD images of base materials (a) ETP-Cu, and (b) SS304L.

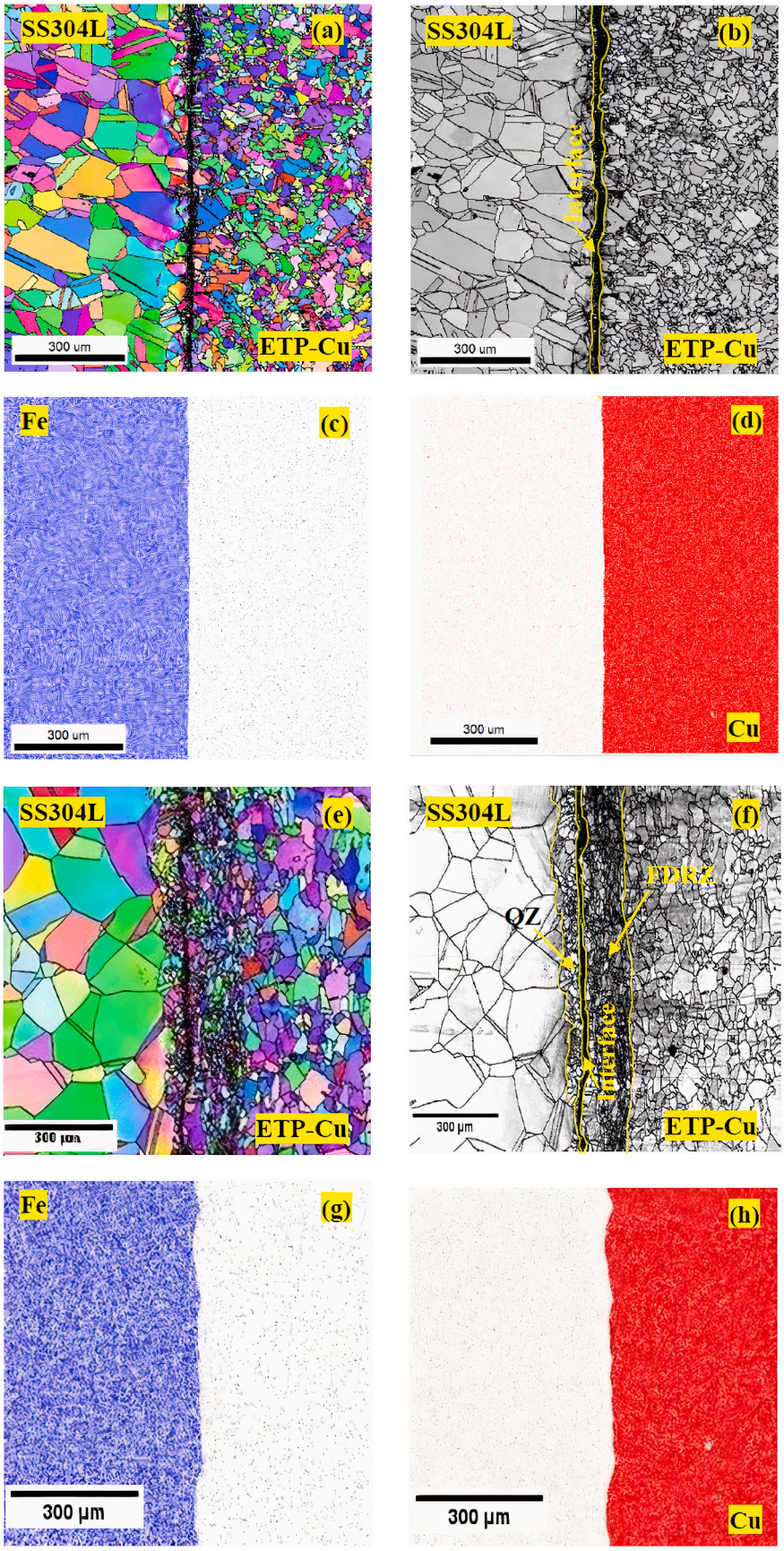

Fig. 8. EBSD images of interface region for weld made by friction time of ((a)&(b)) 10 s, and ((e)&(f)) 15 s; elemental mapping images for weld made by friction time of ((c)&(d))10 s corresponding to images of ((a)&(b)) and ((g)&(h)) 15 s corresponding to images of ((e)&(f)).

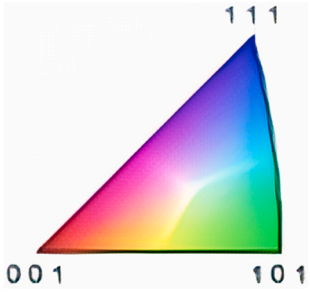

Fig. 9. IPF map image for EBSD shown in Fig. 7.

side to the interface of weld made by friction time of 10 s is 17.39 μm and the same is observed as 13.47 μm in case of weld made by friction time of 15 s, whereas the average grain size of SS side to the interface is observed as 29.07 μm in case of weld made by friction time of 10 s and the same is observed as 23.21 μm in case of friction time of 15 s. The decreased average grains size at SS and Cu sides can be correlated with Fig. 8 (e)&(f), wherein grain refinement is distinctly observed at the interface region. Therefore, this grain refinement after dynamic recrystallization is resulted in decreased average grain size in case of weld made by friction time of 15 s.

Fig. 12 shows SEM and EDX images with line mapping across Cu-SS interface of weld made by friction time of 15 s. It can be seen that elements of Fe and Cu are interacting at the interface region, which confirms the elemental diffusion at the interface and that in turn resulted into enhanced bonding between Cu and SS. The diffusion between elements is occurred due to thermo-mechanical processing on chemically active surfaces under the visco-plastic effect of intersecting surfaces of Cu and SS materials.

3.3. Mechanical properties (tensile testing and microhardness measurements) and fracture surface inspection on post tensile tested specimens

Fig. 13 shows the tensile testing results of ETP-Cu base material and welds of two different conditions such as weld made by 10 s friction time and weld made by 15 s friction time. The values in Fig. 13 shows average values after tensile testing of two specimens from each condition). It can be seen that there is a significant difference in tensile strength and yield strength for welds made under the two aforementioned conditions. In the case of weld made by friction time of 15 s, the maximum ultimate tensile strength (UTS) of 181.05 MPa and maximum yield strength (YS) of 146.17 MPa are obtained. Besides, the UTS of 50.08 MPa and YS of 30.78 MPa are noticed for weld made by friction time of 10 s, which are considered as extremely low strengths as compared to ETP-Cu base material.

Fig. 14 shows the fractured tensile specimens of weld made by friction time of 10 s. It can be seen from Fig. 14 (a) & Fig. 14 (d) that the fracture has occurred from the interface between Cu and SS in both the tensile fractured specimens. In Fig. 14, Cu and SS can be distinguished seen at the outer surfaces. Only at the center region of these fractured surfaces, some Cu material can be seen at SS side fractured surfaces (Fig. 14 (c) and Fig. 14 (f)), which shows that partial metallurgical bonding only occurs at the center region of the cross-section, and out surfaces are observed weakest. Therefore, the fracture is possibly initiated from the outer surface and propagated towards the center. Fig. 15 shows the fractured surface photograph by scanning electron microscopy, which shows a flat surface at the Cu side (Fig. 15 (a)) and some broken grains from the SS side (Fig. 15 (b)). Also, some precipitates are observed on the fractured surface image of the SS side (Fig. 15 (b)) that are possibly IMCs or Cu material bonded to SS in a discontinuous manner. Overall, in this weld made by friction time of 10 s, the fractured surfaces indicate brittle fracture with flat surfaces.

Fig. 16 shows the fractured tensile specimens of weld made by

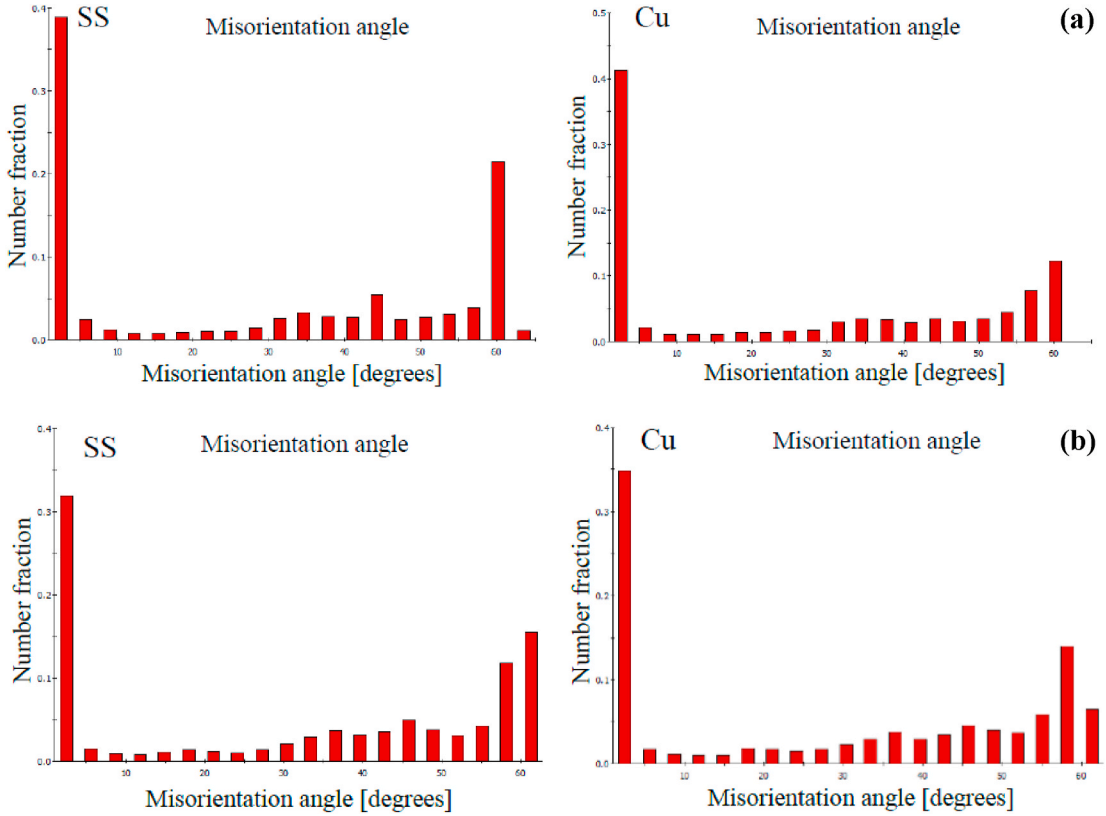

Fig. 10. Grain misorientation angle corresponding to Fig. 8; (a) weld made by friction time of 10 s, and (b) weld made by friction time of 15 s.

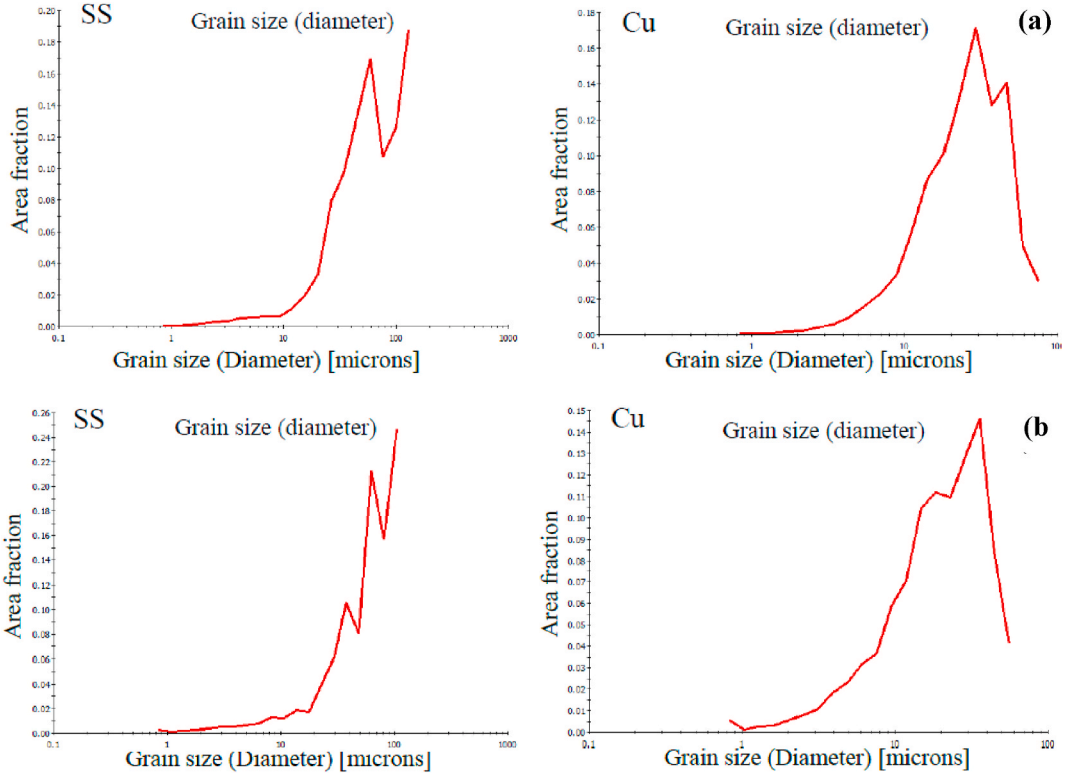

Fig. 11. Grain size measurement (in microns) of welded joints made by (a) friction time of 10 s and (b) friction time of 15 s.

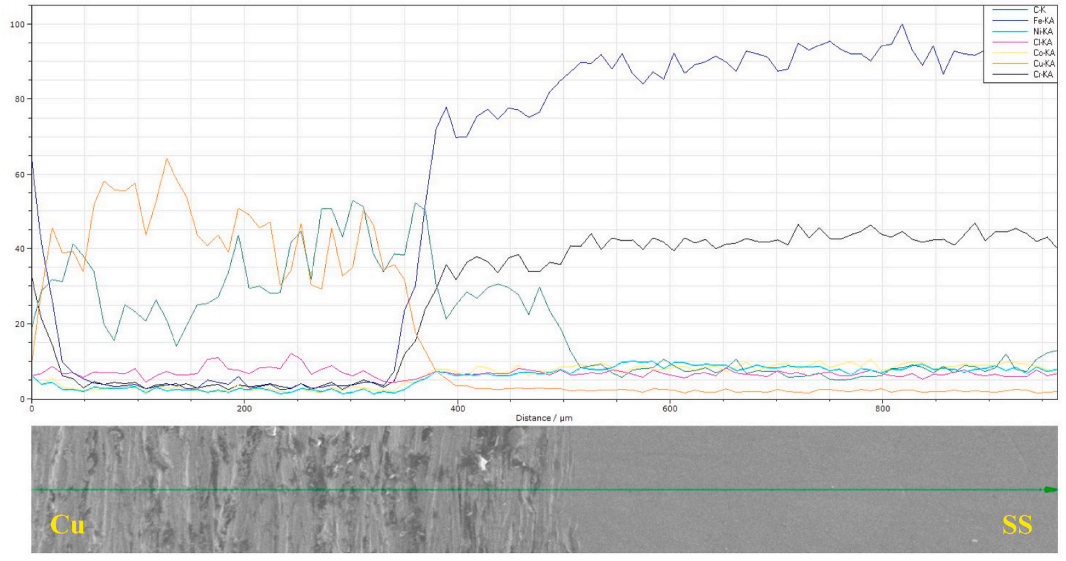

Fig. 12. SEM and EDX images with line mapping for Cu-SS interface of weld made by friction time of 15 s.

friction time of 15 s. It can be seen from Fig. 16 (a) & Fig. 16 (d) that the fracture has occurred from the interface between Cu and SS in both the tensile fractured specimens (like it is observed in Fig. 15 (a) & Fig. 15 (d)). However, the thick layer of Cu is stuck to the SS surface that can also be seen from Fig. 16 (c) & Fig. 16 (f). In Fig. 16, Cu can be seen at both the fractures surfaces of the Cu side as well as the SS side. Based on this it can be confirmed that Cu and SS are metallurgically welded but possibly fractured from either reaction layer of interface region or reaction layer-Cu interface. The fractured surfaces are interpreting as ductile fractures as they are consisting of broken grains having dimples as can be seen from SEM images shown in Fig. 17. Also, these dimples are observed on the Cu side (Fig. 17 (a) and 17 (b)) as well as the SS side (Fig. 17 (c) & Fig. 17 (d)), because the fracture is initiated from the metallurgically bonded region and ended at metallurgically bonded Cu on SS. As the Cu material has experienced severe plastic deformation and has formed recrystallized grains at Cu side near to the interface region (as evidenced in previous sections), it can be correlated that the same is responsible for ductile fracture for fractured tensile specimens for Cu-SS weld made by friction time of 15 s.

Fig. 18 shows microhardness measurements at every 100 µm distance for Cu-SS welds made by friction time of 10 s and 15 s. It can be seen that there are no major variations in microhardness values

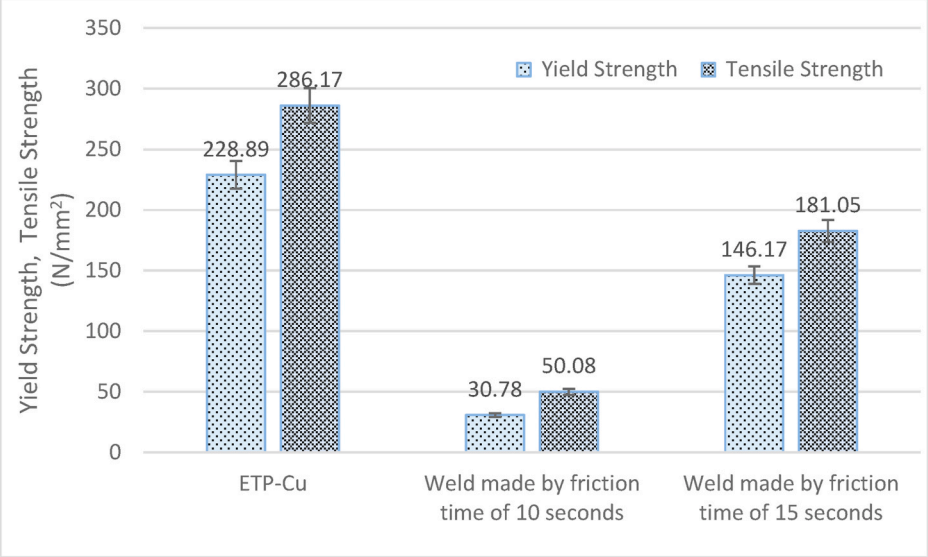

Fig. 13. Tensile strength and yield strength of ETP- Cu base materials and Cu-SS welds made for two different conditions.

observed for welds made by friction time of 10 s and 15 s. On the Cu side, the mean microhardness value is noted as 63.2 HV and 61.1 HV for welds made by friction time of 10 s and 15 s, respectively. No distinct variations in microhardness measurements for PDRZ and HAZ regions are observed as these zones are not evidenced with significant changes in microstructures as compared to the base material of ETP-Cu.

4. Discussion

Based on the obtained results and referred literature [1,2,5–25], it can be stated that the welding of dissimilar pipe materials such as Cu to SS by friction welding is more complicated than similar materials welding because of different thermo-physical properties and inevitably in the chemistry of each metal. The discussion part is presented as follows in the same sequence of above presented results.

4.1. Microstructure (optical microscopy)

During friction welding, the Cu pipe has formed severe flashes at the edge of the pipe and the same has not been observed at SS pipe (refer Fig. 2), because of the same reason of thermo-mechanical action on two different materials. The Cu has a very limited energy loss that helps plastic metal deformation, and thus causes more flash than the SS [17]. Due to the same reason, the microstructural changes are majorly observed at the Cu side under thermo-mechanical action caused by friction welding. Besides, no distinct variation in microstructure is observed on the SS side, as SS is stronger than Cu. Upon friction welding, the base materials experience viscoplastic material behavior and that is higher in the case of Cu as compared to SS, which in turn influences larger changes in microstructures at the Cu side as compared to the SS side. However, small QZ is identified at SS side. This QZ is very small in width as compared to other microstructure zones observed at the Cu side, because the SS side is less affected under applied thermo-mechanical action as compared to the Cu side. In the case of weld made by friction time of 10 s (refer Fig. 4 (f)), the QZ is observed relatively thick but non-continuous as compared to the same observed for weld made by friction time of 15 s (refer Fig. 5 (c)). This is may be because better interdiffusion occurred in the case of welds made by friction time of 15 s as compared to weld made by friction time of 10 s.

It can be interpreted that this variation is due to differences in friction time that subsequently influenced the thickness of reaction layers. As mentioned earlier that, these reaction layers are formed may be due to oxide formation or formation of IMCs [9,13,24–27]. Therefore, here, in this case, it can be expected that the higher friction time (for instance 15 s) have benefitted to reduce this undesirable layer of oxide formation at the interface, due to better reactions on chemically active surfaces of Cu and SS that is governed by higher friction time (of 15 s). The higher friction time can lead to higher thermo-mechanical combined action and this favorable action, in turn, activates chemically active surfaces for interatomic diffusion bonding, where most of the oxides are expected to be removed along with flash in case of friction welding. Besides, the oxides are not able to be removed in case of weld made by friction time of 10 s. On the other side, it may happen this layer is of IMCs. In the case of weld made by a higher friction time of 15 s, the materials' consolidation at the interface is observed better as compared to weld made by friction time of 10 s. This in turn may also have affected the formation of IMCs, and consolidation of the IMCs layer, which has resulted in reduced thickness of IMCs.

In the microstructures, the differences in PDRX and FDRZ are observed in Figs. 4 and 5, because of different processing conditions of welds by two different friction times. Weld made by friction time of 15 s has allowed more time to lead fully recrystallized zone with materials consolidation at the interface region, whereas weld made by friction time of 10 s have not limitedly consolidated material at the interface with more flash formation. This in turn has resulted in a more pronounced FDRZ formation for weld made by 15 s. In general, for both the welds, the FDRZ is mainly formed at the center region of the thickness's cross-section, towards the Cu side of the Cu-SS interface. At FDRZ, full dynamic recrystallization has occurred because this zone is close to the rubbing action where it experiences high heat (with temperature expecting higher than the recrystallization temperature of Cu) and materials deformation due to axial pressure [22,24]. As compared to SS, Cu is soft and hence FDRZ has occurred at the Cu side near to the interface region. Besides, PDRZ has formed away from the FDRZ region where the affection of heat (expected to be less than a recrystallized temperature of Cu) and material deformation are less as compared to the interface region. Also, the Cu had a better plastic deformation behavior compared with SS material [24]; which leads to some areas with PDRZ being identified within this zone (as shown in Figs. 4(f) and 5(a)).

4.2. EBSD analysis at the interface zone, SEM and EDX

EBSD results have confirmed that the thermo-mechanical processing has affected the interface region's grains with clear and distinct grains

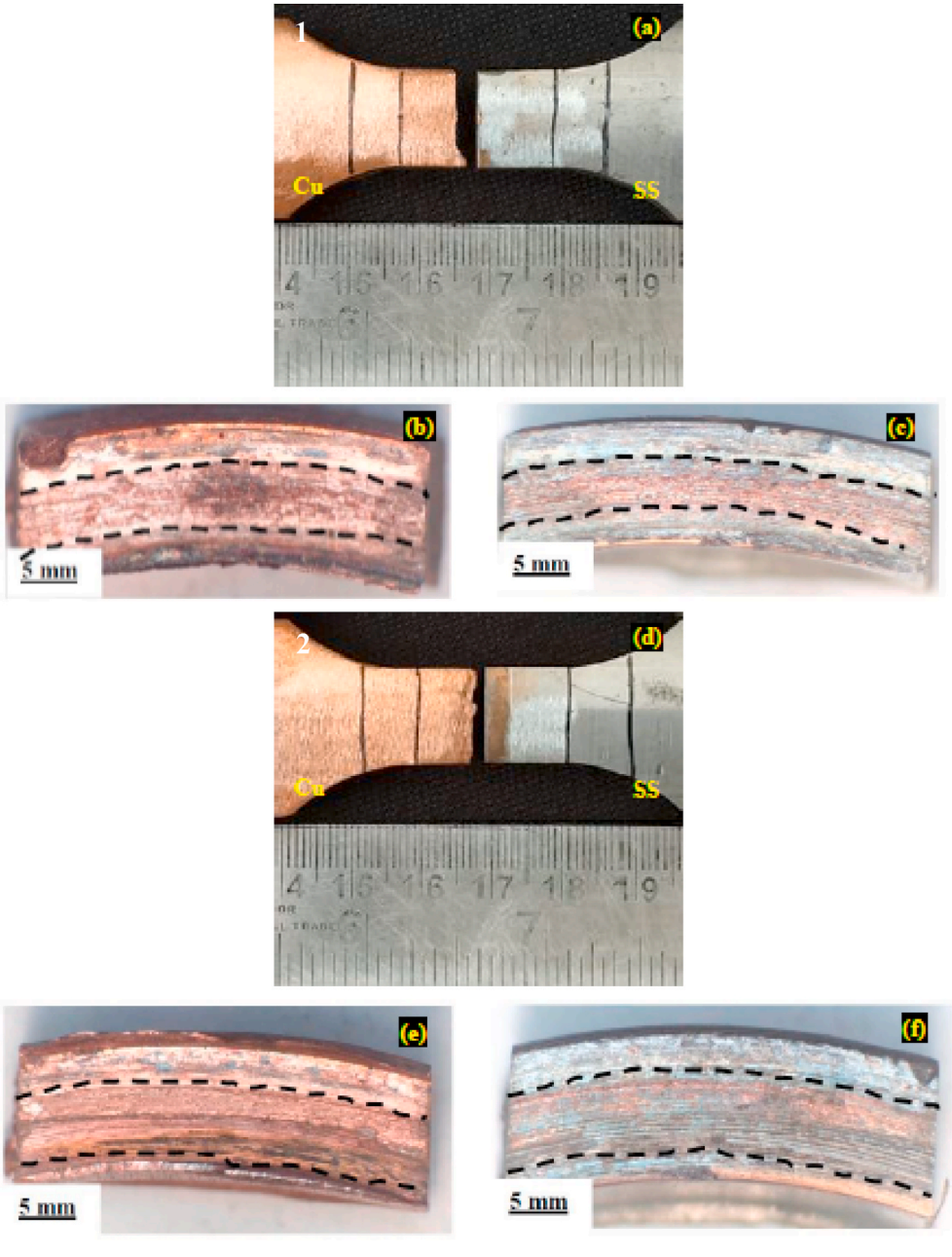

Fig. 14. Fracture location after tensile testing and fracture surface images at a macroscopic level for weld made by friction time of 10 s. (a) broken tensile specimen (tensile specimen 1), (b) fractured surface of Cu side for broken specimen shown in (a), (c) fractured surface of SS side for broken specimen shown in (a), (d) broken tensile specimen (tensile specimen 2), (e) fractured surface of Cu side for broken specimen shown in (d), (f) fractured surface of SS side for broken specimen shown in (d).

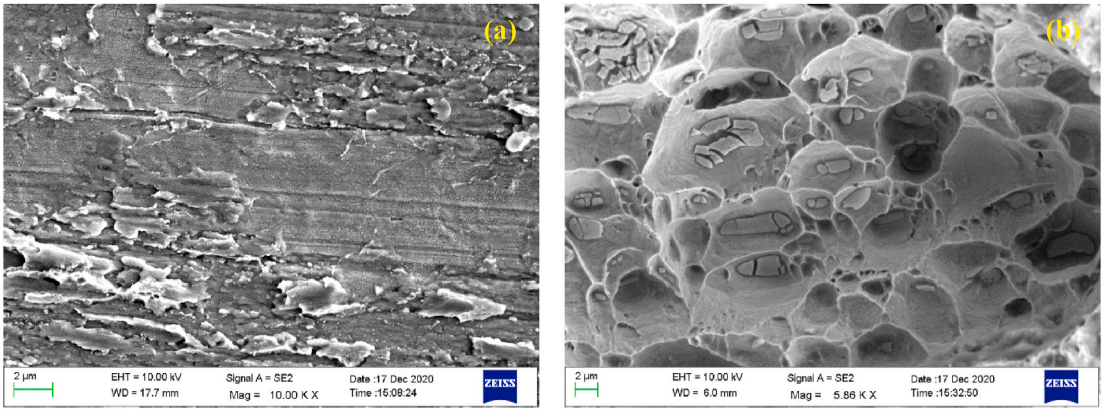

Fig. 15. SEM images of the fracture surfaces of tensile tested weld made by friction time of 10 s (a) Cu side, (b) SS side.

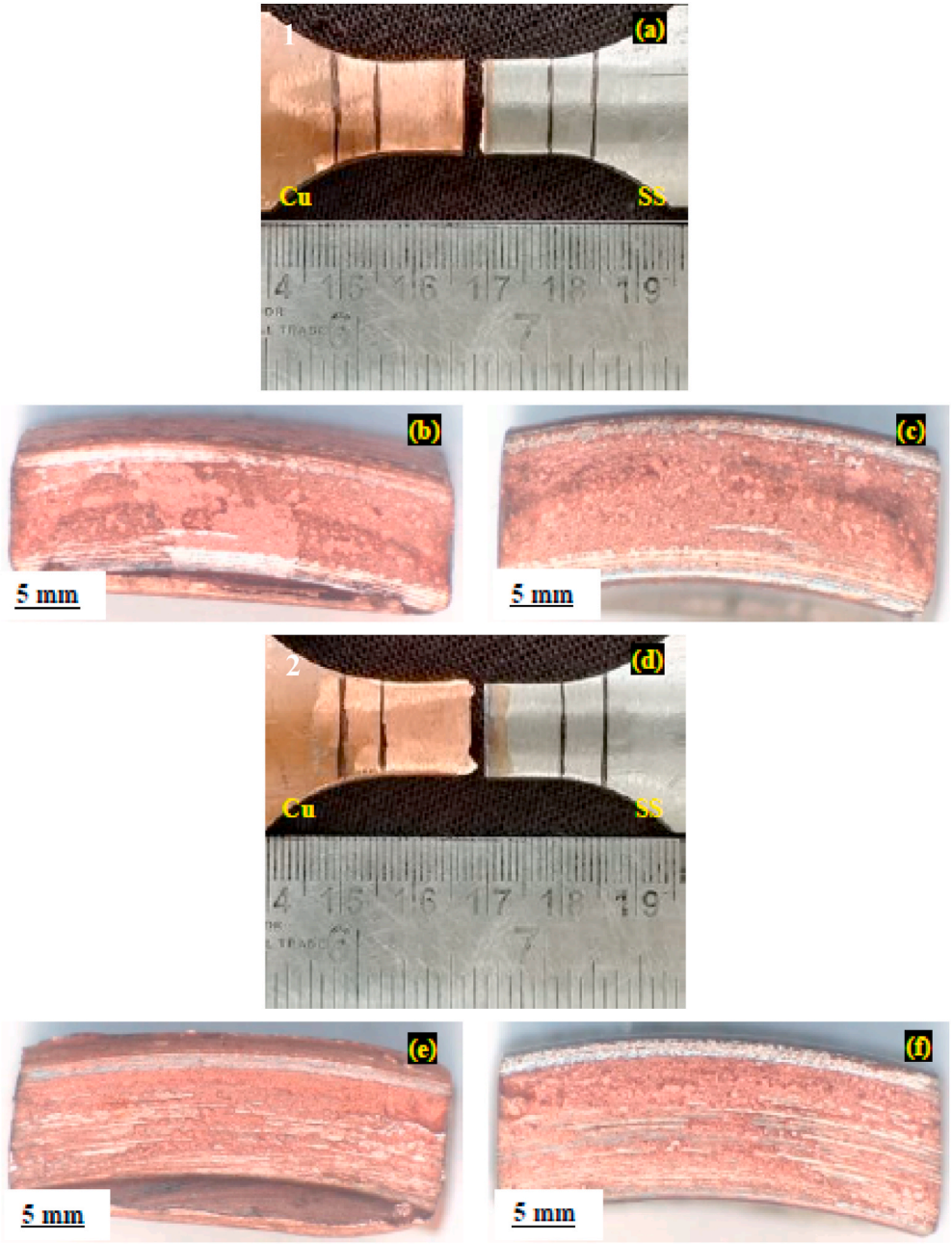

Fig. 16. Fracture location after tensile testing and fracture surface images at a macroscopic level for weld made by friction time of 15 s. (a) broken tensile specimen (tensile specimen 1), (b) fractured surface of Cu side for broken specimen shown in (a), (c) fractured surface of SS side for broken specimen shown in (a), (d) broken tensile specimen (tensile specimen 2), (e) fractured surface of Cu side for broken specimen shown in (d), (f) fractured surface of SS side for broken specimen shown in (d).

near the interface region. Similar EBSD results are also observed in literature of [7]. The distinction in grain evolution between both the conditions such as welds made by two different friction times is also confirmed, which shows differences in thermo-mechanical processing and their influence on microstructure evolution. It is possible to state that inadequate thermo-mechanical processing between Cu and SS materials is evidenced in case of weld made by friction time of 10 s, as no distinct microstructural changes at the interface such as FDRZ and/or QZ are observed, whereas adequate thermo-mechanical processing between Cu and SS materials is evidenced in case of weld made by friction time of 15 s with district FDRZ at Cu side and QZ at SS side. Friction time has significant influence on thermo-mechanical processing that has resulted in differences in grains evolution for both conditions. With EBSD results of elemental distribution as can be seen in Fig. 8 (c)&(d) and Figure (g)&(h), it can be confirmed that the significant dynamic recrystallization at interface region has resulted in interface with wave-like intermixing of materials (with elemental diffusion) in case of weld made by friction time of 15 s (refer Fig. 8 (g)&(h)), whereas the same is not so significant to influence grains and elements at the interface region in case of weld made by friction time of 10 s (refer Fig. 8 (c)&(d)). Therefore, it can be stated that the adequate interfacial materials mixing is obtained in weld made by friction time of 15 s through wave-like elemental distribution at interface, which has occurred due to better intermixing in visco-plastic domain of materials at the interface. Further, in EBSD analysis, there are more variations in misorientation angles and grain size observed in the case of weld made by friction time of 15 s as compared to weld made by friction time of 10 s. This is may be because of the significant transformation of grains (through continuous dynamic recrystallization) in case of weld made by friction time of 15 s that is already observed as significant at the interface region (refer Fig. 8 (e)&(f)), as compared to the same in case of weld made by friction time of 10 s (refer Fig. 8 (a)&(b))., It can also be said that the weld of higher friction time of 15 s leads to more strain accretion in the materials as compared to the weld of lower friction time of 10 s and that in turn

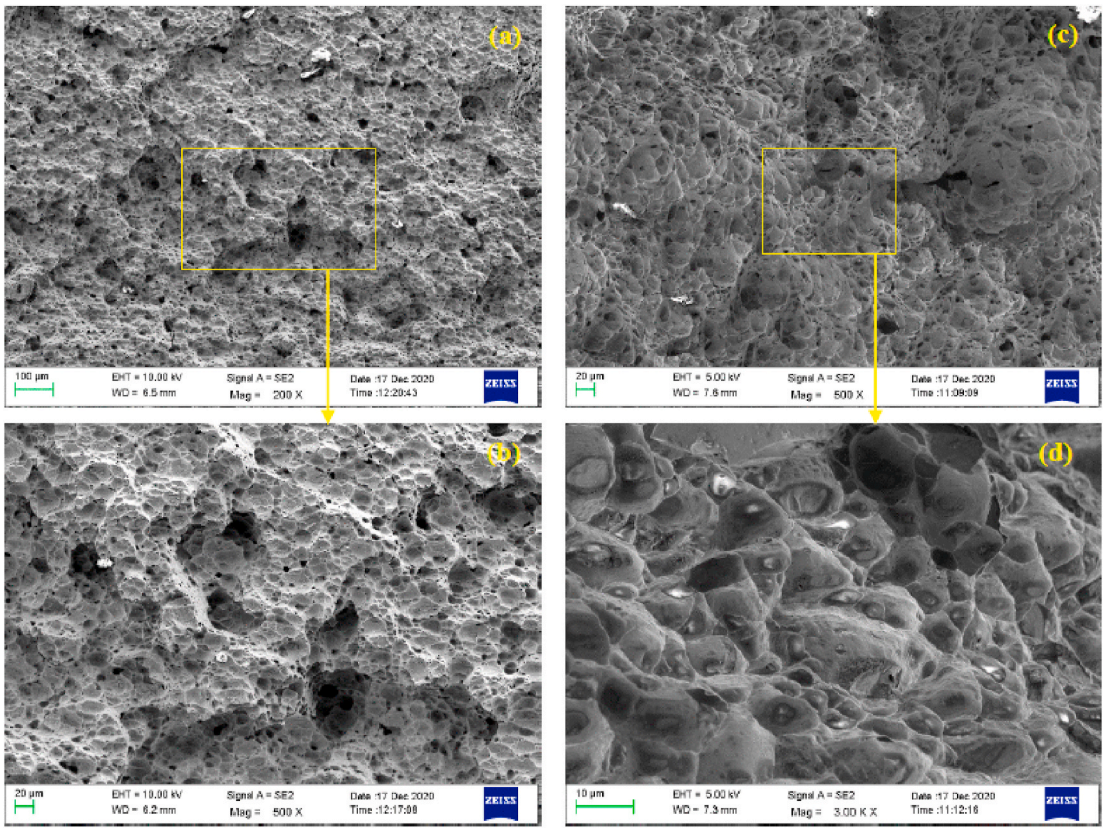

Fig. 17. SEM images of the fracture surfaces of tensile tested weld made by friction time of 10 s (a & b) Cu side and (c & d) SS side.

resulted in lower grain size at interface region in case of weld of higher friction time of 15 s. Also, the higher friction time of 15 s has increased the heat generation with severe plastic deformation and enhanced the grain growth.

Fig. 19 shows the XRD of weld made by friction time of 15 s. It can be seen that along with Fe and Cu, IMCs such as $FeCu_4$ and Cu_9Si have been interpreted based on peaks and International Centre for Diffraction Data card. The same IMCs are also claimed in the literature of [24]. This confirms interatomic diffusion between Fe–Cu elements and Cu–Si elements, which is occurred under thermo-mechanical action caused during friction welding between Cu and SS materials. It can be stated that the formation of new crystalline phase reforms after the interatomic diffusion between Fe and Cu, and Cu and Si. The formation of IMCs affects mechanical properties; for instance, the Cu_9Si of IMC is weaker in strength that in turn leads to lower joint strength. But, the formation of $FeCu_4$ can enhance joint strength [24].

Figs. 12 and 19 are evidencing effective bonding with intermixing at the interface region of Cu-SS weld made by friction time of 15 s, and this supports the claims that are made in previous discussions based on microstructural observations.

4.3. Mechanical properties (tensile testing and microhardness measurements) and fracture surface inspection on post tensile tested specimens

It can be correlated from previous results and discussions on interface analysis of Cu-SS weld made by friction time of 10 s that extremely low strengths are noticed because of poor bonding observed in this case, wherein interatomic diffusion and materials mixing between Cu-SS are observed as poor. Besides, in case of Cu-SS weld made by friction time of 15 s, better metallurgical condition of improved materials mixing with adequate interatomic diffusion is evidenced in microstructural and interface analysis section, which in turn resulted in increased tensile and yield strengths as compared to weld made by friction time of 10 s. Despite better intermixing, the joint efficiency of around 63% is observed as compared to ETP-Cu in the case of weld made by friction time of 15 s that may be because of formation of IMCs and oxides at the. In the literature of dissimilar materials friction welds, joint strength is usually observed lower than base material because of the formation of IMCs or other reaction layers at the interface [5–26]. In the fractured tensile specimens, the fractured surfaces show fracture from reaction layer. Better intermixing between Cu and SS is evidenced in the fractured tensile specimen of weld made by friction time of 15 s. In another study of [22] for Cu-SS pipe welds, the joint efficiency is observed 80% of Cu material, wherein pipe thickness is 5.6 mm. In the present investigation, the pipe thickness is 3.6 mm that means that the contact area during FW is lower than that of in case of [22]. This could be the reason for lower joint efficiency as compared to Ref. [22]. Besides, further optimization of processing conditions can be considered to improve joint efficiency.

A minor reduction of microhardness at Cu side near to interface is observed for weld made by friction time of 15 s as compared to weld made by friction time of 10 s (at FDRZ region). This is due to grain refinement evidenced in microstructural analysis at the FDRZ region near to interface side at Cu (as discussed in previous sections). At the interface region towards the SS side, the microhardness is observed higher than the same observed for SS base material. This is due to the combined effect of developed grains with solid solution strengthening at the diffusion line [24], and formation of IMCs at the interface, or any of single reason from these reasons [25–27]. The microhardness at the interface region (i.e. QZ region) towards the SS side is observed as 182.3 HV and 179.02 HV for the welds of friction time 10 s and 15 s respectively. Even though, there are microstructural changes observed for the QZ region for the welds of friction time 10 s and 15 s, no major variations in microhardness are observed in the QZ. This is because QZ's thickness is very thin, and indentation may have occurred even bigger than QZ's

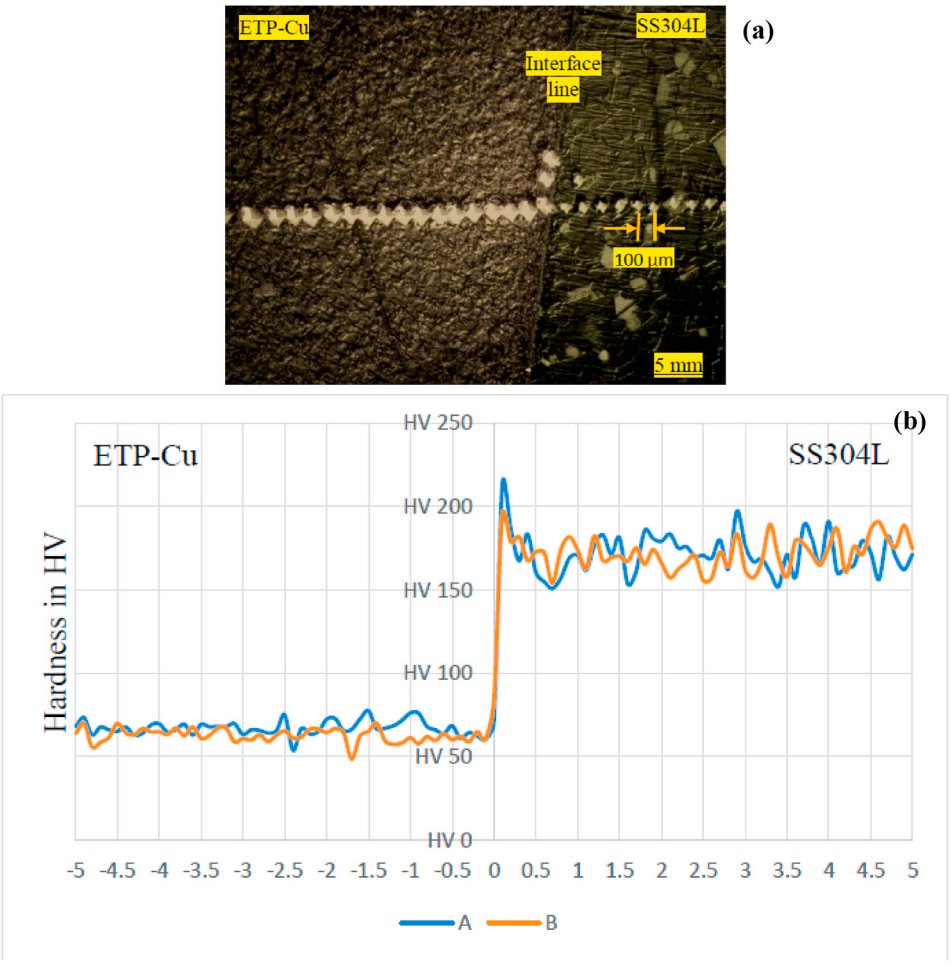

Fig. 18. (a) Image showing indentations for microhardness measurements on weld made by friction time of 15 s and (b) microhardness measurements at every at 100 µm distance for Cu-SS welds made by friction time of 10 s (shown by line A) and 15 s (shown by line B).

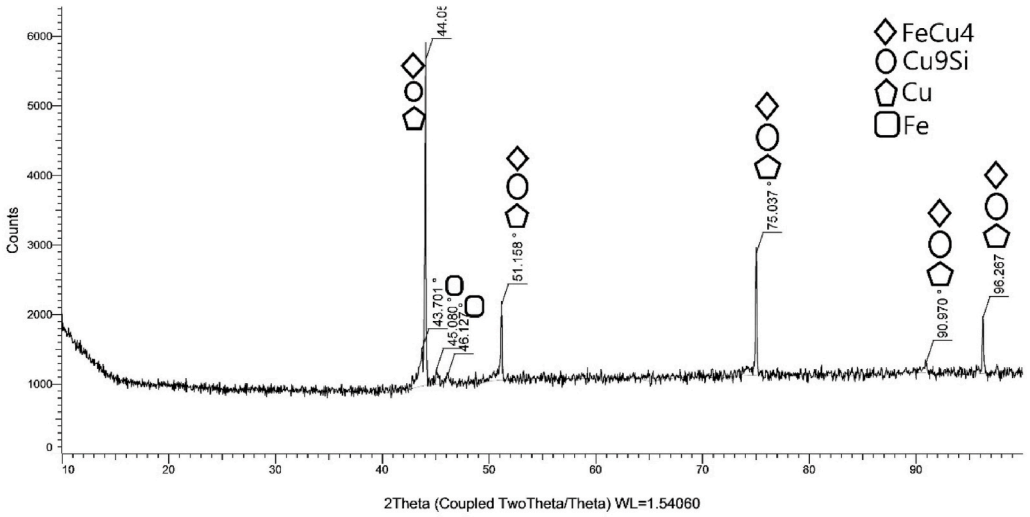

Fig. 19. XRD test for the phase identification for weld made by friction time of 15 s.

thickness. No other significant variations in microhardness at the SS side are observed that can be correlated with no significant microstructural changes at the SS side. Similar results are also observed in the literature of [26].

5. Conclusion

The present study investigates microstructure evolution and mechanical properties of dissimilar Cu-SS pipe joints welded by continuous drive friction welding under two different processing conditions (by

varying friction times of 10 s and 15 s, while keeping other processing parameters constant). Interesting results are observed, and the following specific conclusion can be made.

- The microstructural evolution in dissimilar materials Cu-SS friction welds is influenced by the processing condition of friction times. Major microstructural variations are observed at the Cu side with different microstructure evolution such as full dynamic recrystallized zone, partial dynamic recrystallized zone, and heat-affected zone, wherein the full dynamic recrystallized zone is clearly and distinctly observed very close to Cu-SS interface at Cu side. Quenching zone with refined grains is observed at SS side very close to Cu-SS interface. This microstructural evolution is clearly defined in the case of weld made by friction time of 15 s, whereas the same is not developed in case of weld made by friction time of 10 s.
- Enhanced metallurgical bonding between Cu-SS materials is observed with microstructural variations (such as full dynamic recrystallized zone at Cu side and quenching zone at SS side) near to Cu-SS interface, in case of weld made by friction time of 15 s. Superior interatomic diffusion leading to enhanced metallurgical bonding is evidenced in this study for weld made by friction time of 15 s.
- The reaction layer thickness influences the bonding and mechanical properties of Cu-SS friction welds. The reaction layer thickness of 17.28 μm is observed for the weld made by friction time of 10 s, whereas the reaction layer thickness of 1.21 μm is observed for the weld made by friction time of 15 s. The ultimate tensile strength of 181.05 MPa with 63% of joint efficiency as compared to ETP-Cu base material is obtained for Cu-SS friction weld made by friction time of 15 s. The hardness measurement variations are observed at the interface region of Cu-SS welds due to grain refinements at these locations.

CRediT authorship contribution statement

Hardik D. Vyas: Investigation, Methodology, Resources, Experimentation, Formal analysis, Writing – original draft. **Kush P. Mehta:** Conceptualization, Formal analysis, Funding acquisition, Methodology, Project administration, Resources, Supervision, Validation, Visualization, Writing – review & editing. **Vishvesh Badheka:** Discussions, Project administration, Resources, Funding acquisition, Participation in meetings, Technical support, Supervision. **Bharat Doshi:** Supervision, Project collaborator.

Declaration of competing interest

The authors declare that they have no known competing financial interests or personal relationships that could have appeared to influence the work reported in this paper.

Acknowledgments

Funding for this research by the Board of Research in Nuclear Sciences, India (Project No: 39/14/02/2018-BRNS/39002) and support for experimental assistance by Vulcan Industrial Engineering are sincerely acknowledged.

References

[1] K.P. Mehta, A review on friction-based joining of dissimilar aluminum-steel joints, J. Mater. Res. 34 (2019) 78–96, https://doi.org/10.1557/jmr.2018.332.
[2] M. Aritoshi, K. Okita, Friction welding of dissimilar metals, Weld. Int. 17 (2003) 271–275, https://doi.org/10.1249/01.mss.0000538518.76078.fa.
[3] W. Li, A. Vairis, M. Preuss, T. Ma, Linear and rotary friction welding review, Int. Mater. Rev. 61 (2016) 71–100, https://doi.org/10.1080/09506608.2015.1109214.
[4] M.B. Uday, M.N.A. Fauzi, H. Zuhailawati, A.B. Ismail, Advances in friction welding process: a review, Sci. Technol. Weld. Join. 15 (2010) 534–558, https://doi.org/10.1179/136217110X12785889550064.
[5] H. Vyas, K.P. Mehta, V. Badheka, B. Doshi, Pipe-to-pipe friction welding of dissimilar Al-SS joints for cryogenic applications, J. Brazilian Soc. Mech. Sci. Eng. 42 (2020), https://doi.org/10.1007/s40430-020-2181-1.
[6] K.P. Mehta, V.J. Badheka, A review on dissimilar friction stir welding of copper to aluminum: process, properties, and variants, Mater. Manuf. Process. 31 (2016) 233–254, https://doi.org/10.1080/10426914.2015.1025971.
[7] N. Gotawala, A. Shrivastava, Investigation of interface microstructure and mechanical properties of rotatory friction welded dissimilar aluminum-steel joints, Mater. Sci. Eng. 825 (2021) 141900, https://doi.org/10.1016/j.msea.2021.141900.
[8] K.P. Mehta, V.J. Badheka, Effects of tilt angle on the properties of dissimilar friction stir welding copper to aluminum, Mater. Manuf. Process. 31 (2016) 255–263, https://doi.org/10.1080/10426914.2014.994754.
[9] R. Beygi, R.J.C. Carbas, A.Q. Barbosa, E.A.S. Marques, L.F.M. da Silva, A comprehensive analysis of a pseudo-brittle fracture at the interface of intermetallic of η and steel in aluminum/steel joints made by FSW: microstructure and fracture behavior, Mater. Sci. Eng. 824 (2021) 141812, https://doi.org/10.1016/j.msea.2021.141812.
[10] K. Mehta, A. Astarita, P. Carlone, R. Della Gatta, H. Vyas, P. Vilaça, F. Tucci, Investigation of exit-hole repairing on dissimilar aluminum-copper friction stir welded joints, J. Mater. Res. Technol. (2021), https://doi.org/10.1016/j.jmrt.2021.06.019.
[11] H. Zhang, K.X. Jiao, J.L. Zhang, J. Liu, Microstructure and mechanical properties investigations of copper-steel composite fabricated by explosive welding, Mater. Sci. Eng. 731 (2018) 278–287, https://doi.org/10.1016/j.msea.2018.06.051.
[12] P. Sahlot, S.S. Nene, M. Frank, R.S. Mishra, A. Arora, Towards attaining dissimilar lap joint of CuCrZr alloy and 316L stainless steel using friction stir welding, Sci. Technol. Weld. Join. 23 (2018) 715–720, https://doi.org/10.1080/13621718.2018.1499186.
[13] M.P. Satpathy, A. Kumar, S.K. Sahoo, Effect of brass interlayer sheet on microstructure and joint performance of ultrasonic spot-welded copper-steel joints, J. Mater. Eng. Perform. 26 (2017) 3254–3262, https://doi.org/10.1007/s11665-017-2772-x.
[14] C. Shanjeevi, S.S. Kumar, P. Sathiya, Multi-objective optimization of friction welding parameters in AISI 304L austenitic stainless steel and copper joints, Proc. Inst. Mech. Eng. Part B J. Eng. Manuf. 230 (2016) 449–457, https://doi.org/10.1177/0954405414555590.
[15] C. Shanjeevi, S. Satish Kumar, P. Sathiya, Evaluation of mechanical and metallurgical properties of dissimilar materials by friction welding, Procedia Eng. 64 (2013) 1514–1523, https://doi.org/10.1016/j.proeng.2013.09.233.
[16] L. Fu, S.G. Du, Effects of external electric field on microstructure and property of friction welded joint between copper and stainless steel, J. Mater. Sci. 41 (2006) 4137–4142, https://doi.org/10.1007/s10853-006-6224-5.
[17] J. Luo, X. Wang, D. Liu, F. Li, J. Xiang, Inertia radial friction welding joint of large size H90 brass/D60 steel dissimilar metals, Mater. Manuf. Process. 27 (2012) 930–935, https://doi.org/10.1080/10426914.2011.610087.
[18] M. Sahin, Joining of stainless steel and copper materials with friction welding, Ind. Lubric. Tribol. 61 (2009) 319–324, https://doi.org/10.1108/00368790910988435.
[19] K. Tsuchiya, H. Kawamura, Mechanical properties of Cu-Cr-Zr alloy and SS316 joints fabricated by friction welding method, J. Nucl. Mater. 233–237 (1996) 913–917.
[20] G. Vairamani, T.S. Kumar, S. Malarvizhi, V. Balasubramanian, Application of response surface methodology to maximize tensile strength and minimize interface hardness of friction welded dissimilar joints of austenitic stainless steel and copper alloy, Trans. Nonferrous Met. Soc. China (English Ed. 23 (2013) 2250–2259, https://doi.org/10.1016/S1003-6326(13)62725-9.
[21] H.D. Vyas, K.P. Mehta, V. Badheka, B. Doshi, Processing and evaluation of dissimilar Al-SS friction welding of pipe configuration: nondestructive inspection, properties, and microstructure, Meas. J. Int. Meas. Confed. 167 (2021) 108305, https://doi.org/10.1016/j.measurement.2020.108305.
[22] H.D. Vyas, K.P. Mehta, V. Badheka, B. Doshi, Friction welding of dissimilar joints copper-stainless steel pipe consist of 0.06 wall thickness to pipe diameter ratio, J. Manuf. Process. 68 (2021) 1176–1190, https://doi.org/10.1016/j.jmapro.2021.06.050.
[23] J. Luo, J. Xiang, D. Liu, F. Li, K. Xue, Radial friction welding interface between brass and high carbon steel, J. Mater. Process. Technol. 212 (2012) 385–392, https://doi.org/10.1016/j.jmatprotec.2011.10.001.
[24] Y. Wang, J. Luo, X. Wang, X. Xu, Interfacial characterization of T3 copper/35CrMnSi steel dissimilar metal joints by inertia radial friction welding, Int. J. Adv. Manuf. Technol. 68 (2013) 1479–1490, https://doi.org/10.1007/s00170-013-4936-7.
[25] P. Patel, H. Rana, V. Badheka, V. Patel, W. Li, Effect of active heating and cooling on microstructure and mechanical properties of friction stir–welded dissimilar aluminium alloy and titanium butt joints, Weld. World 64 (2020) 365–378, https://doi.org/10.1007/s40194-019-00838-6.
[26] M. Kimura, K. Ohara, M. Kusaka, K. Kaizu, K. Hayashida, Effects of tensile strength on friction welding condition and weld faying surface properties of friction welded joints between pure copper and austenitic stainless steel, J. Adv. Join. Process. 2 (2020) 100028, https://doi.org/10.1016/j.jajp.2020.100028.
[27] G. Thirunavukarasu, V.V. Patel, S. Kundu, A. Alankar, Diffusion bonding of Ti6Al4V and SS 304 with Nb interlayer, Mater. Perform. Char. 8 (5) (2019) 1008–1031. https://www.astm.org/mpc20190041.html.